http://dx.doi.org/10.5012/bkcs.2013.34.5.1401

Protein Structural Characterization by Hydrogen/Deuterium Exchange Mass Spectrometry with Top-down Electron Capture Dissociation

Hai Dong Yu,[†,‡] Seonghee Ahn, and Byungjoo Kim[†,*]

[†]*Korea Research Institute of Standards and Science, Daejeon 305-340, Korea.* [*]*E-mail: byungjoo@kriss.re.kr*
[‡]*University of Science & Technology, Daejeon 305-350, Korea*
Received December 27, 2012, Accepted February 8, 2013

This study tested the feasibility of observing H/D exchange of intact protein by top-down electron capture dissociation (ECD) mass spectrometry for the investigation of protein structure. Ubiquitin is selected as a model system. Local structural information was obtained from the deuteration levels of c and $z^{\cdot}$ ions generated from ECD. Our results showed that α-helix region has the lowest deuteration level and the C-terminal fraction containing a highly mobile tail has the highest deuteration level, which correlates well with previous X-Ray and HDX/NMR analyses. We studied site-specific H/D exchange kinetics by monitoring H/D exchange rate of several structural motives of ubiquitin. Two hydrogen bonded β-strands showed similar HDX rates. However, the outer β-strand always has higher deuteration level than the inner β-strand. The HDX rate of the turn structure (residues 8-11) is lower than that of β-strands (residues 1-7 and residues 12-17) it connects. Although isotopic distribution gets broader after H/D exchange which results in a limited number of backbone cleavage sites detected, our results demonstrate that this method can provide valuable detailed structural information of proteins. This approach should also be suitable for the structural investigation of other unknown proteins, protein conformational changes, as well as protein-protein interactions and dynamics.

Key Words : FT-ICR MS, Top-down, Electron capture dissociation, Hydrogen deuterium exchange, Protein structure

Introduction

Hydrogen/deuterium exchange (HDX) combined with mass spectrometry (MS) has become a powerful tool for the study of protein structure and dynamics in solution, because HDX behavior of a protein reflects its overall structural characteristics and conformational flexibility.[1-4] When an intact protein is incubated in D_2O, amide hydrogens on the protein surface or in unstructured regions can be exchanged with deuterium within several seconds, while those buried within the hydrophobic core or those involved in hydrogen bonding (especially in the regions of β-sheet or α-helix) will not exchange unless changes in structure expose them to solvent and hydrogen bonding is perturbed. So, the propensity of hydrogen to exchange provides information on the conformational properties of a folded protein in solution phase.[1]

There are two kinds of HDX labeling methods for introducing deuterium into a protein: pulse labeling and continuous labeling.[5] In pulse labeling method, after a protein is subject to perturbations for inducing some kind of conformational change, it is exposed to deuterium for a quick pulse. Then deuterium exchange is quenched by reducing the pH and temperature. Pulse labeling is very effective for the characterization of folding intermediates.[6-10] In continuous labeling method, protein is directly exposed to D_2O. At a series of time points, an aliquot of the labeled protein is removed and then quenched by reducing pH and temperature. Continuous labeling is very useful for the determination of slow unfolding transitions and most unfolding events in proteins. It also can provide detailed information on protein dynamics, as well as local and global stability.[11-14] Continuous labeling is more commonly used compared to pulse labeling, because continuous labeling is technically simpler to perform.

Traditionally, hydrogen exchange has been measured by NMR spectroscopy.[15-17] However, large proteins (greater than ~35 kDa) are generally not suitable for NMR analysis,[18] which is the major limitation of NMR. In a recent development, mass spectrometry (MS) is employed for the determination of the level of HDX in certain locations of a target protein, because MS can determine proteins that are beyond the NMR size limit. Compared to NMR, mass spectrometric methods present greater sensitivity and higher throughput. Also, MS can be used for identification of unknown proteins in complex mixtures. Relatively small amount of sample is required in mass spectrometric methods.[19]

A large number of studies have been reported on the feasibility of gas-phase fragmentation methods used in MS/MS for determining deuterium incorporation, without peptic digestion. Unfortunately, most MS/MS strategies may cause deuterium scrambling prior to or during dissociation. The majority of previous work has been based on collision-induced dissociation (HDX/CID). Some reports showed some retaining of spatial deuteration patterns in HDX/CID studies.[20-25] However, others showed apparent scrambling resulted from CID in HDX/MS/MS studies.[26-29] Even though it has been reported that another threshold dissociation

method, infrared multiphoton dissociation (IRMPD),[30,31] causes little or no deuterium scrambling in HDX-MS,[32] the labile modifications are lost prior to backbone cleavage, thus making it difficult to identify the modification site. Recently, Polfer and co-workers have reported abundant NH_3 and H_2O losses from b fragments when employing IRMPD in HDX studies and they also reported that SORI CID (sustained off-resonance irradiation collision-induced dissociation)[33] can cause more scrambling products and internal fragments.[34]

Of those fragmentation methods, electron capture dissociation (ECD) is a promising alternative, where a multiply-protonated protein ion, trapped in a Fourier transform-ion cyclotron resonance (FT-ICR) cell,[35] captures a low-energy electron at a protonated site, leading to N-C_α cleavage and producing c and z$^{\cdot}$ ions by a nonergodic process.[36,37] In HDX-MS, the advantage of ECD is that bond cleavage during ECD proceeds faster than intramolecular H migration because ECD occurs faster than energy randomization.[36,38] Therefore, information of labile post-translational modifications could be retained. Jørgensen and co-workers have proved that ECD can preserve solution-phase deuteration pattern of short peptides, their results showed that only limited amide hydrogen migration occurs upon ECD.[39] Furthermore, compared to threshold techniques such as IRMPD and CID, diversity of backbone sites are cleaved in ECD. There is less backbone cleavage selectivity in ECD, and therefore ECD can provide a larger sequence coverage, which facilitates the analysis of intact protein by "top-down" approach.[40] Hagman successfully obtained site-specific HDX information of peptides using top-down ECD.[41] In the report, single residue HDX kinetics was obtained. Several studies have combined ECD with HDX for exploring structural characterization of proteins. Kelleher and co-workers reported HDX-ECD studies of yeast recombinant ubiquitin using signal improvements through depletion of ^{13}C and ^{15}N heavy isotopes, but detailed description of the protein structure was not reported.[42] Recently, Konermann and co-workers have successfully elaborated the structural differences between native holo-myoglobin and apo-myoglobin by using HDX-MS with top-down ECD.[43] They also reported an application of ECD for spatially resolved HDX studies of ubiquitin,[44] in their results, 30 c and 19 z$^{\cdot}$ ions were found with sufficiently high S/N ratios and the deuteration levels of these c and z$^{\cdot}$ ions were consistent with previous HDX-NMR data. However, detailed characterization of ubiquitin structure was not described in their report yet. Moreover, in previous HDX-ECD studies of proteins, few site-specific kinetic studies were reported. Recently, another similar dissociation method, electron transfer dissociation (ETD),[45] was used for top-down MS analysis to probe HDX behavior of ubiquitin. Sterling *et al*. studied H/D exchange in ESI spraying droplet and observed HDX kinetics of several amino acid residues.[46] This article focused on HDX in the presence of a super-charge reagent to study possible structural change of ubiquitin upon ESI and supercharging of the protein. Rand *et al.* studied HDX of side chain hydrogens of ionized ubiquitin in gas phase, and structural information was obtained from site-specific HDX levels.[47]

This work uses bovine ubiquitin as a model system for investigating the feasibility of studying protein structure by continuous labeling HDX-MS with top-down ECD. Ubiquitin is a small cytoplasmic protein which is composed of a mixed β-sheet containing five β-strands, three and one-half turns of α-helix, a short piece of 3_{10} helix, seven reverse turns, and a C-terminal tail (residues 71-76) which is highly flexible and provides no protection from amide exchange (Figure 1).[15,48-50] The native structure of this protein is remarkably resistant to chemical and pH-induced denaturation.[19] Its structure has been well characterized by X-ray crystallography[48,49] and NMR.[50,51] Also, its HDX behavior has been studied by NMR,[15,16] which provides a solid foundation for comparison with HDX-MS. In this study, in order to see if top-down ECD can provide structural information of ubiquitin by monitoring its HDX behavior, ECD was performed to monitor HDX of ubiquitin. The experimental results were compared with ubiquitin structural information which has been well-known. HDX kinetics of several structural motives of ubiquitin was studied to test if more structural information can be obtained.

Materials and Methods

Materials. Bovine ubiquitin (76 residues, MW 8565 Da, no disulfide bond), deuterium oxide (D_2O, 99.9% D), formic acid (FA), were purchased from Sigma-Aldrich (St. Louis, MO, USA) and used without further purification.

Continuous Labeling HDX. HDX was initiated by mixing 1 mM ubiquitin in H_2O with D_2O in a 1:9 volume ratio, which is similar to the method used by Konermann *et al.*.[28] The solution was maintained at room temperature for different times for the H/D exchange to occur. At each designated time point, a 20 μL aliquot was removed from the original tube, quenched with an equal volume of cold 2% FA in D_2O (in an ice bath) and immediately subjected to ESI-FTICR MS. In order to analyze HDX behavior and determine the deuteration levels of ubiquitin, non-deuterated ubiquitin sample was needed for comparison, which was prepared by mixing 100 μL of 100 μM ubiquitin in H_2O with 100 μL of cold 2% FA in H_2O to give a concentration of 50 μM ubiquitin in H_2O (1% FA). A full-deuteration control sample was prepared by keeping the continuous labeling HDX sample at room temperature for 24 hours. Then 20 μL was removed, quenched with an equal volume of cold 2% FA in D_2O and analyzed by ESI-FTICR MS.

Nano ESI-FT-ICR-MS and ECD. All spectra were obtained with a commercial 12-T Fourier transform mass spectrometer (FTMS; Ionspec Inc., Lake Forest, CA, USA) equipped with an ECD capability. Direct infusion of cold-quenched H/D exchange media (D_2O with 1% FA and 5% H_2O as described in section 2.2) was performed with automated chip-based nano-ESI-MS on a Triversa NanoMate 100 system (Advion BioSciences, Ithaca, NY, USA) in positive ion mode. ESI conditions were as follows: gas pressure of 0.5 psi and capillary voltage of 1.8 kV. The flow

rate is dependent on the chip internal diameter. Here, 5.5 μm-ESI chip was used as static nanoelectrospray emitter, providing flow rates between 60 and 250 nL/min. Survey scan data were recorded with an accumulation time of 500 ms in a hexapole linear trap. However, ions were accumulated for a period of 3000 ms prior to injection into ICR cell for ECD. ECD was performed for 300 ms with low-energy electron irradiation from an on-axis indirectly heated dispenser cathode (model STD200, diameter: 3.4 mm; Heatwave Labs, Wastonville, CA, USA). The cathode potential during electron injection was −1 V and was kept at +5 V otherwise. Filament voltage was maintained at 6.0 V, both filament trapping plate and quadrupole trapping plate were held at 10.0 V, inner trapping ring was held at 0.0 V during ECD. The entire ubiquitin ion population was subjected to ECD without precursor selection.

Data Analysis. Figure 1 shows the structure of ubiquitin (PDB ID 1UBI). The secondary structure is as follows: N-terminal β-strand 1-7; turn 8-11; second β-strand 10-17; turn 18-21; α-helix 23-34; turn 37-40; third β-strand 40-45; turn 45-48; fourth β-strand 48-50; turn 51-54; 3_{10}-helix 56-59; turn 57-60; turn 62-65; fifth β-strand 64-72; a highly flexible tail 71-76. Ubiquitin contains a total of 144 labile hydrogens. Of those, 72 are amide backbone hydrogens, 69 are on amino acid side chains, and 3 on the termini. In this study, all of the labile hydrogens are considered. Deuteration levels of molecular ions and fragment ions were calculated from the shift of the average mass of each of their ion cluster.[42]

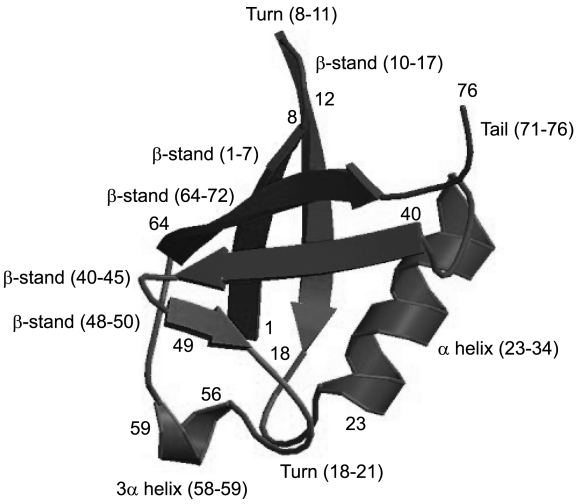

Figure 1. The structure of ubiquitin (PDB ID 1UBI).[55]

Results and Discussion

24 h of Full Deuteration. ECD mass spectra of non-deuterated ubiquitin produced a large number of c and $z^{\cdot}$ ions from extensive backbone cleavages (Figure 2(a)). However, compared to ECD of non-deuterated ubiquitin, a little less number of backbone cleavage sites were detected above signal-to-noise level for ECD of fully deuterated ubiquitin (Figure 2(b)). This is because isotopic distribution gets broader after H/D exchange. 32 c and 23 $z^{\cdot}$ ions were detected from ECD of non-deuterated ubiquitin in this experimental

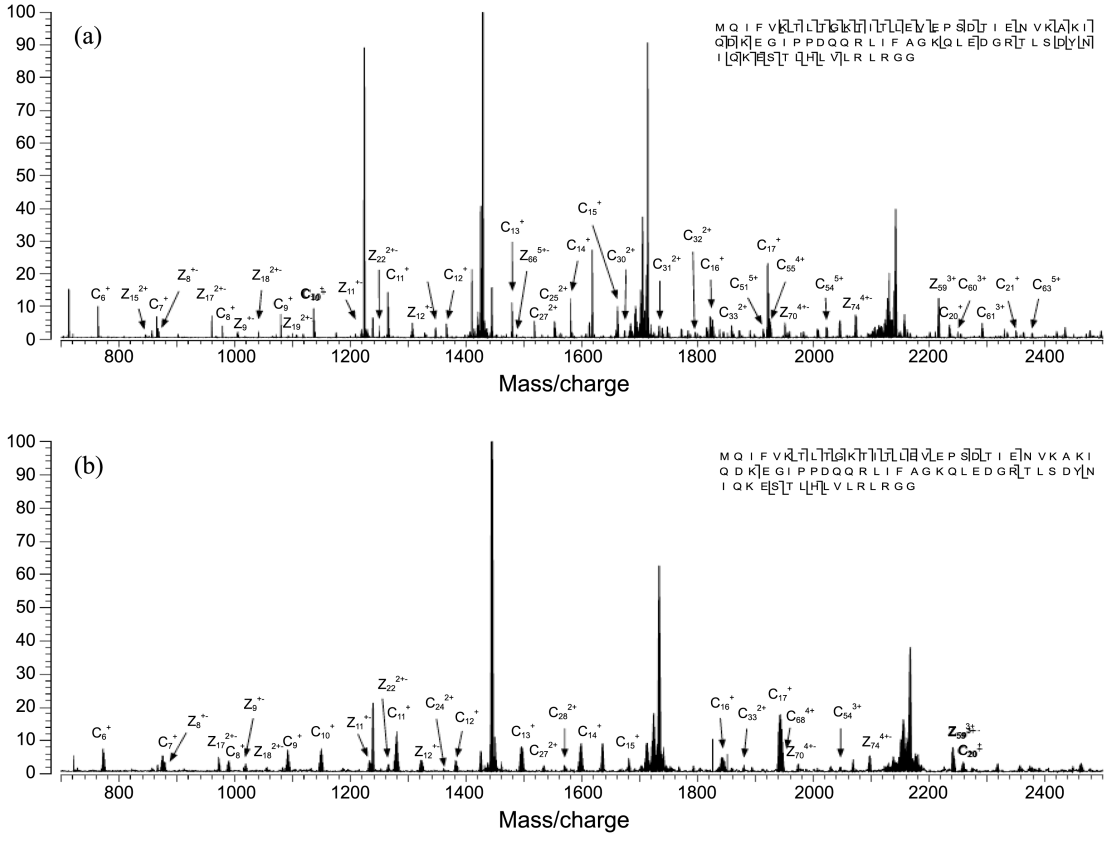

Figure 2. (a) ECD MS spectra of ubiquitin in H_2O. (b) ECD MS spectra of ubiquitin after 24 h of H/D exchange in D_2O.

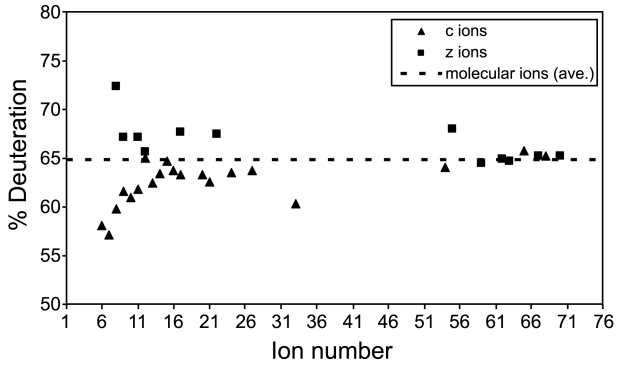

Figure 3. Deuteration levels of c and z· ions of ubiquitin after 24 h H/D exchange in D_2O.

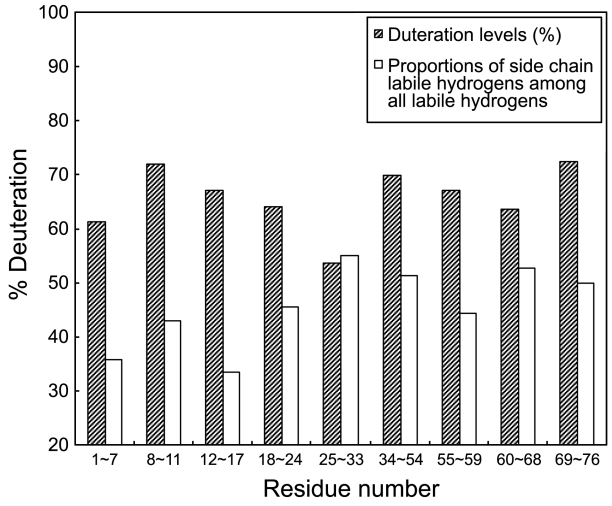

Figure 4. Site-specific H/D exchange levels of ubiquitin after full H/D exchange in D_2O.

condition. After 24-hour full H/D exchange, only 20 c and 12 z· ions were observed with sufficiently high S/N ratios. Molecular ions of 5+ charge state, 6+ charge state and 7+ charge state showed similarly around 65% of overall deutration level. The deuteration level of each detectable c and z· ions is shown in Figure 3. The dash line showed the overall deuteration level of ubiquitin, from averaging the deuteration level of 5+ charge state, 6+ charge state and 7+ charge state molecular ions. In contrast to molecular deuteration level, the deuteration level of C-terminal fraction (short z ions) is higher and the deuteration level of N-terminal fraction (short c ions) is lower. The deuteration of C-terminal fraction is much higher than that of N-terminal fraction, which can be attributed that the C-terminal fraction contains a highly flexible tail (residues 71-76) and N-terminal fraction contains two hydrogen-bonded β-strands (residues 1-7 and residues 10-17) and a tightly packed α-helix (residues 23-34).

Deuterium Content of Each Segment of Ubiquitin. In HDX of proteins, exchangeable hydrogens include the hydrogens attached to heteroatoms in the side chains, three hydrogens on the N- and C- terminal groups (H_2N- and -COOH) and backbone amide hydrogens. In general, hydrogens in the side chains and hydrogen on the terminal groups are known to exchange rapidly, however, backbone amide hydrogens are known to have a variety of isotopic exchange rates depending on the environment around each backbone amide.[21] In folded proteins, some backbone amide hydrogens exchange relatively quickly while others exchange slowly. In some case, it is known to take several months for amide hydrogens exchange depending on their 3-D structure.[4] In this study, local HDX properties of ubiquitin were obtained after 24 h of HDX reaction to test if structural information of the protein can be obtained. HDX levels of structural motives in ubiquitin were estimated from deuteration levels of detectable c and z· ions shown in Figure 3. Figure 4 shows deutration levels of structurally important segments of ubiquitin. For comparison, the proportion of side chain labile hydrogens (including C- and N-terminus hydrogens) in overall labile hydrogens in each segment was shown as a reference value in Figure 4. The deuteration levels of segments (in residues 1-54) which are close to N-terminal, are calculated by using c ions, and the deuteration levels of segments (in residues 55-76) which are close to C-terminal, are calculated by using z· ions. As shown in Figure 4, residues 25-33 showed the lowest deuteration level, which is close to its reference value. This is in accord with its structural characteristics, as residues 25-33 has α-helix structure. Backbone amide hydrogens of this α-helix segment are protected and only labile side chain hydrogens can be exchanged. In helix structure, the side chains are on the outside of the helix. So, these labile hydrogens on the side chains are almost unprotected. However, backbone amide hydrogens are protected through hydrogen bonding with carboxyl groups and undergo little HDX. Deuteration levels of other segments are higher than their reference values, indicating that parts of hydrogens in amide groups are exchanged with deuteriums. Residues 1-7 and residues 12-17 have β-strand structure and these two adjacent β-strands are hydrogen bonded each other in a mixed β-sheet (see Figure 1). Segments for residues 12-17 and residues 1-7 have higher deuteration levels than their corresponding reference values, indicating that backbone amide hydrogens in β-strands are not well protected compared to those in α-helix. The results could be due to weaker interaction of amide hydrogen of a β-strand to carbonyl oxygen of the other β-strand compared to hydrogen interaction of amide hydrogen and adjacent carbonyl oxygen in α-helix. This postulation is consistent with the ubiquitin structure shown in Figure 1, where the two β-strands are not perfectly parallel to each other and the hydrogen interactions may not be stronger than those in α-helix. Residues 8-11 that has a turn structure and lies on the protein surface, connecting two β-strands (residues 1-7 and residues 12-17), shows much higher deuteration level. The segment for residues 69-76 shows the highest deuteration level, which can be attributed that this segment contains a highly flexible tail (residues 71-76). Due to a less number of cleavage sites are detected after 24 h deuteration, many segments (shown in Figure 4) contains more than one structural motif. For example, residues 18-24 contains a turn

(residues 18-21) and a small portion of α-helix (residues 23-24), residues 69-76 contains a portion of β-strand (residues 69-72) and a tail (residues 71-76), *etc*. It is difficult to characterize these segments only from their H/D exchange behavior.

Besides ubiquitin native structure, ubiquitin has a famous A-state structure which refers to a partially denatured ubiquitin structure in the presence of acid and organic co-solvent. According to articles[53,54] reporting ubiquitin A-state, only minimal changes were observed in MS spectra when methanol concentration was varied within the 0-30% range and the presence of 30-70% methanol could lead to three ubiquitin conformers. In our experimental conditions, instead of using organic solvent, only water solution with 1% formic acid was used in order to minimize denaturation and ensure native state structure. Therefore, the "A-state" issue was not considered in this study.

HDX Kinetics. Figure 5 shows overall deuteration levels of ubiquitin molecular ions as a function of time. Ubiquitin molecular ions at charge states of +4, +5, +6, and +7 showed similar HDX kinetics. ECD is performed to try to monitor HDX kinetics of segments containing structural mortifs of ubiquitin. However, due to the broadening of isotopic distribution after H/D exchange, only a limited number of ions are detected at all time points for reliable assignment. Here, a few segments are chosen to probe HDX kinetics of structural motives of ubiquitin. As shown in Figure 6, the exchange rate for residues 1-7 is nearly equal to that for residues 12-17, which is in accordance with their structural characteristics, as they both have β-strand structure and these two β-strands are hydrogen bonded to each other in the β-sheet. The lower deuteration level of residues 1-7 than that of residues 12-17 is attributed that residues 1-7 is inner strand and residues 12-17 is outer strand in the β-sheet. The initial deuteration levels of these three segments are compared with their corresponding reference values (in Figure 4), proportions of side chain labile hydrogens among all labile hydrogens in those segments. We find that the initial deuteration level of residues 1-7 is lower than its reference value in Figure 4, indicating that labile hydrogens on the side chains of residues 1-7 are not completely exchanged at the instant HDX period as this β-strand segment lies inside the β-sheet. However, the initial deuteration levels of residues 8-11 and residues 12-17 are both higher than their reference values in Figure 4, indicating that labile hydrogens on the side chains of these segments are mostly exchanged instantly and parts of backbone amide hydrogens of these segments have been exchanged at the instant HDX period. Here, the initial deuteration time was typically about 10s to finish the quenching procedure. The initial deuteration level of residues 8-11 is highest, which is in accordance with the secondary structural characteristics and the location of residues 8-11, a turn on the surface. These findings further support the structural characteristics of these segments. However, the slope of the plot for residues 8-11 is smaller than that for residues 1-7 or residues 12-17. We attribute this phenonmenon to an especially stable antiparallel G1 β-bulge of the turn (residues 7-11) which stabilize the N-teriminal β-hairpin of ubiquitin (residues 1-17). Labile hydrogens on sides chains of the turn exchange instantly as soon as HDX occurs, however, backbone amide hydrogens involved in the bulge of the turn (Gly10, Lys11 and Thr7) exchange slowly.[48,52]

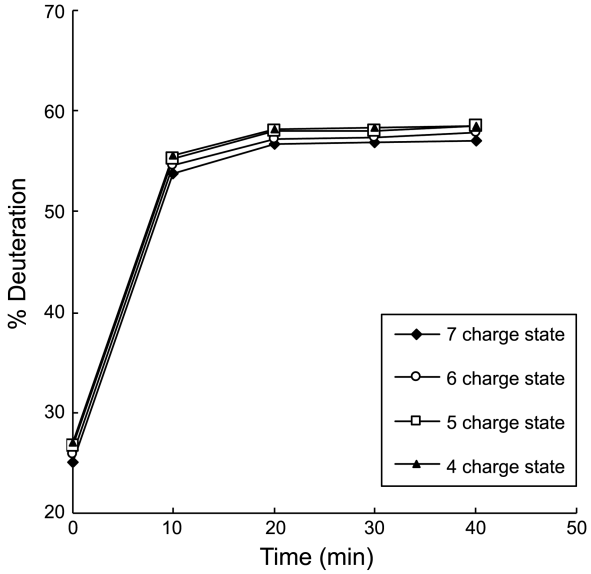

Figure 5. Deuteration levels of ubiquitin molecular ions as a function of time.

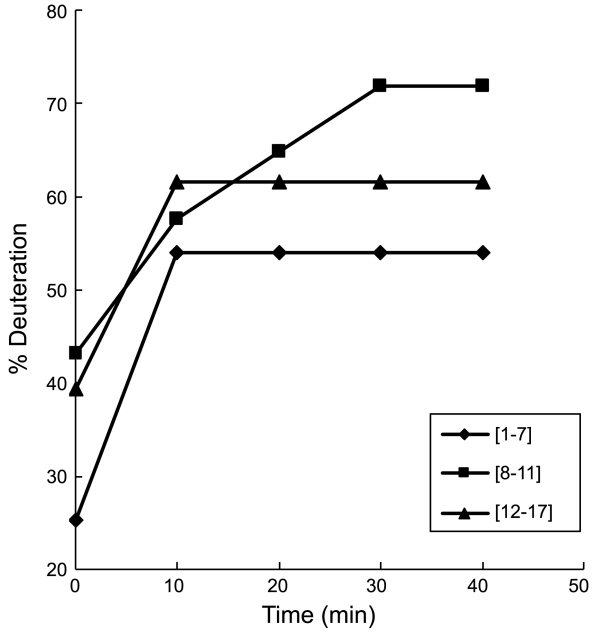

Figure 6. Deuteration levels in a few sequential segments of ubiquitin as a function of time.

Conclusions

In this study, we selected ubiquitin, a well-known protein, as a model system for probing protein structural information by using HDX-MS with Top-down ECD. The obtained HDX-MS data from Top-down ECD were compared with the structural properties of the protein to see if HDX-MS with

ECD can provide structural information for the protein. Also, site-specific HDX kinetics of ubiquitin was obtained using Top-down ECD which was little reported in previous studies. Our data showed that the deuteration level of C-terminal fraction (short $z^{\cdot}$ ions) is higher than that of the N-terminal fraction (short c ions) after 24 h full H/D exchange, which is attributed that C-terminal fraction contains a highly flexible tail (residues 71-76) and N-terminal fraction contains two hydrogen-bonded β-strands (residues 1-7 and residues 10-17) and a tightly packed α-helix (residues 23-34). The α-helix region showed the lowest deuteration level, and the turn (residues 8-11) on the surface of the protein that connects two adjacent β-strands showed very high deuteration level. These obtained HDX features of the structural motives are consistent with the structural features obtained by X-Ray and previous HDX/NMR data. Our data also showed that similar structural motives (β-strands) have similar HDX kinetics which can reflect ubiquitin dynamics and structural information. In summary, this work showed that ECD product ions can successfully provide detailed protein structural characteristics by determining their HDX behavior, which validates the feasibility of this approach for the study of protein structure in solution.

Acknowledgments. This work was supported by the Korea Research Institute of Standards and Science under projects 'Establishment of standard system in organic analysis (grant No.: 13011023) and 'Establishment of standard system in protein analysis (grant No.: 13011017).

References

1. Garcia, R. A.; Pantazatos, D.; Villarreal, F. J. *ASSAY and Drug Development Technologies* **2004**, *2*, 81-91.
2. Wagner, D. S.; Melton, L. G.; Yan, Y. B.; Erickson, B. W.; Anderegg, R. J. *Protein Sci.* **1994**, *3*, 1305-1314.
3. Kragelund, B. B.; Robinson, C. V.; Knudsen, J.; Dobson, C. M.; Poulsen, F. M. *Biochemistry* **1995**, *34*, 7217-7224.
4. Wales, T. E.; Engen, J. R. *Mass Spectrometry Reviews* **2006**, *25*, 158-170.
5. Deng, Y.; Zhang, Z.; Smith, D. L. *J. Am. Soc. Mass Spectrom.* **1999**, *10*, 675-684.
6. Krishna, M. M. G.; Hoang, L.; Lin, Y.; Englander, S. W. *Methods* **2004**, *34*, 51-64.
7. Uzawa, T.; Nishimura, C.; Akiyama, S.; Ishimori, K.; Takahashi, S.; Dyson, H. J.; Wright, P. E. *Proc. Natl. Acad. Sci. U.S.A.* **2008**, *105*, 13859-13864.
8. Kuwata, K.; Shastry, R.; Cheng, H.; Hoshino, M.; Batt, C. A.; Goto, Y.; Roder, H. *Nat. Struct. Biol.* **2001**, *8*, 151-155.
9. Roder, H.; Elove, G. A.; Englander, S. W. *Nature* **1988**, *335*, 700-704.
10. Udgaonkar, J. B.; Baldwin, R. L. *Nature* **1988**, *335*, 694-699.
11. Engen, J. R.; Smithgall, T. E.; Gmeiner, W. H.; Smith, D. L. *Biochemistry* **1997**, *36*, 14384-14391.
12. Bai, Y.; Sosnick, T. R.; Mayne, L.; Englander, S. W. *Science* **1995**, *269*, 192-197.
13. Carulla, N.; Barany, G.; Woodward, C. *Biophys. Chem.* **2002**, *101-102*, 67-79.
14. Parker, M. J.; Marqusee, S. *J. Mol. Biol*. **2001**, *305*, 593-602.
15. Pan, Y.; Briggs, M. S. *Biochemistry* ***1992***, *31*, 11405-11412.
16. Bougault, C.; Feng, L.; Glushka, J.; Kupce, E.; Prestegard, J. H. *J. Biomol. NMR* **2004**, *28*, 385-390.
17. Dyson, H. J.; Wright, P. E. *Chem. Rev.* **2004**, *104*, 3607-3622.
18. Yu, H. *Proc. Natl. Acad. Sci. USA.* **1999**, *96*, 332-334.
19. Katta, V.; Chait, B. T. *J. Am. Chem. Soc.* **1993**, *115*, 6317-6321.
20. Anderegg, R. J.; Wagner, D. S.; Stevenson, C. L.; Borchardt, R. T. *J. Am. Soc. Mass Spectrom.* **1994**, *5*, 425-433.
21. Akashi, S.; Naito, Y.; Takio, K. *Anal. Chem.* **1999**, *71*, 4974-4980.
22. Deng, Y.; Pan, H.; Smith, D. L. *J. Am. Chem. Soc.* **1999**, *121*, 1966-1967.
23. Kim, M.-Y.; Maier, C. S.; Reed, D. J.; Deinzer, M. L. *J. Am. Chem. Soc.* **2001**, *123*, 9860-9866.
24. Demmers, J. A. A.; Rijkers, D. T. S.; Haverkamp, J.; Killian, J. A.; Heck, A. J. R. *J. Am. Chem. Soc.* **2002**, *124*, 11191-11198.
25. Cai, X.; Dass, C. *Rapid Commun. Mass Spectrom.* **2005**, *19*, 1-8.
26. Jørgensen, T. J. D.; Gårdsvoll, H.; Ploug, M.; Roepstorff, P. *J. Am. Chem. Soc.* **2005**, *127*, 2785-2793.
27. Ferguson, P. L.; Pan, J.; Wilson, D. J.; Dempsey, B.; Lajoie, G.; Shilton, B.; Konermann, L. *Anal. Chem.* **2007**, *79*, 153-160.
28. Ferguson, P. L.; Konermann, L. *Anal. Chem.* **2008**, *80*, 4078-4086.
29. McLafferty, F. W.; Guan, Z.; Haupts, U.; Wood, T. D.; Kelleher, N. L. *J. Am. Chem. Soc.* **1998**, *120*, 4732-4740.
30. Polfer, N. C. *Chem. Soc. Rev.* **2011**, *40*, 2211-2221.
31. Eyler, J. R. *Mass Spectrom. Rev.* **2009**, *28*, 448-467.
32. Hofstadler, S. A.; Sannes-Lowery, K. A.; Griffey, R. H. *J. Mass Spectrom.* **2000**, *35*, 62-70.
33. Gauthier, J. W.; Trautman, T. R.; Jacobson, D. B. *Anal. Chim. Acta* **1991**, *246*, 211-225.
34. Tirado, M.; Rutters, J.; Chen, X.; Yeung, A.; Maarseveen, J.; Eyler, J. R.; Berden, G.; Oomens, J.; Polfer, N. C. *J. Am. Soc. Mass Spectrom.* **2012**, *23*, 475-482.
35. Barrow, M. P.; Burkitt, W. I.; Derrick, P. J. *Analyst* **2005**, *130*, 18-28.
36. Zubarev, R. A.; Kelleher, N. L.; McLafferty, F. W. *J. Am. Chem. Soc.* **1998**, *120*, 3265-3266.
37. Kleinnijenhuis, A. J.; Duursma, M. C.; Breukink, E.; Heeren, R. M. A.; Heck, A. J. R. *Anal. Chem.* **2003**, *75*, 3219-3225.
38. Breuker, K.; Oh, H.; Lin, C.; Carpenter, B. K.; McLafferty, F. W. *Proc. Natl. Acad. Sci. U.S.A.* **2004**, *101*, 14011-14016.
39. Rand, K. D.; Adams, C. M.; Zubarev, R. A.; Jørgensen, T. J. D. *J. Am. Chem. Soc.* **2008**, *130*, 1341-1349.
40. Ge, Y.; Lawhorn, B. G.; ElNaggar, M.; Strauss, E.; Park, J.-H.; Begley, T. P.; McLafferty, F. W. *J. Am. Chem. Soc.* **2002**, *124*, 672-678.
41. Hagman, C.; Tsybin, Y. O.; Hakansson, P. *Rapid Commun. Mass Spectrom.* **2006**, *20*, 661-665.
42. Charlebois, J. P.; Patrie, S. M.; Kelleher, N. L. *Anal. Chem*. **2003**, *75*, 3263-3266.
43. Pan, J.; Han, J.; Borchers, C. H.; Konermann, L. *J. Am. Chem. Soc.* **2009**, *131*, 12801-12808.
44. Pan, J.; Han, J.; Borchers, C. H.; Konermann, L. *J. Am. Chem. Soc.* **2008**, *130*, 11574-11575.
45. Zehl, M.; Rand, K. D.; Jensen, O. N.; Jørgensen, T. J. D. *J. Am. Chem. Soc.* **2008**, *130*, 17453-17459.
46. Sterling, H. J.; Williams, E. R. *Anal. Chem*. **2010**, *82*, 9050-9057.
47. Rand, K. D.; Pringle, S. D.; Morris, M.; Brown, J. M. *Anal. Chem*. **2012**, *84*, 1931-1940.
48. Vijay-Kumar, S.; Bugg, C. E.; Cook, W. J. *J. Mol. Biol.* **1987**, *194*, 531-544.
49. Vijay-Kumar, S.; Bugg, C. E.; Wilkinson, K. D.; Cook, W. J. *Proc. Natl. Acad. Sci. U. S. A.* **1985**, *82*, 3582-3585.
50. Briggs, M. S.; Roder, H. *Proc. Natl. Acad. Sci. U. S. A.* **1992**, *89*, 2017-2021.
51. Di Stefano, D. L.; Wand, A. J. *Biochemistry* **1987**, *26*, 7272-7281.
52. Chen, P.; Gopalacushina, B. G.; Yang, C.; Chan, S. I.; Evans, P. A. *Protein Science* **2001**, *10*, 2063-2074.
53. Mohimen, A.; Dobo, A.; Hoerner, J. K.; Kaltashov, I. A. *Anal. Chem*. **2003**, *75*, 4139-4147.
54. Liu, Z.; Cheng, S.; Gallie, D. R.; Julian, R. R. *Anal. Chem*. **2008**, *80*, 3846-3852.
55. Image from the RCSB PDB (www.pdb.org) of PDB ID 1UBI: Ramage, R.; Green, J.; Muir, T. W.; Ogunjobi, O. M.; Love, S.; Shaw, K. *Biochem. J.* **1994**, *299*, 151-158.